A Genomic Model for the Prediction of Ultraviolet Inactivation Rate Constants for RNA and DNA Viruses

Wladyslaw J. Kowalski[1], William P. Bahnfleth[2], Mark T. Hernandez[3]

[1]Immune Building Systems, Inc., 575 Madison Ave., 10th Floor, New York, NY10022, drkowalski@ibsix.com
[2]The Pennsylvania State University, Department of Architectural Engineering, University Park, PA 16802
[3]University of Colorado, UCB 428, Department of Civil, Environmental, and Architectural Engineering, 1111 Engineering Drive #441, Boulder, CO 80309

Abstract

A mathematical model is presented to explain the ultraviolet susceptibility of viruses in terms of genomic sequences that have a high potential for photodimerization. The specific sequences with high dimerization potential include doublets of thymine (TT), thymine-cytosine (TC), cytosine (CC), and triplets composed of single purines combined with pyrimidine doublets. The complete genomes of 49 animal viruses and bacteriophages were evaluated using base-counting software to establish the frequencies of dimerizable doublets and triplets. The model also accounts for the effects of ultraviolet scattering. Constants defining the relative lethality of the four dimer types were determined via curve-fitting. A total 77 water-based UV rate constant data sets were used to represent 22 DNA viruses. A total of 70 data sets were used to represent 27 RNA viruses. Predictions are provided for dozens of viruses of importance to human health that have not previously been tested for UV susceptibility.

Key Words

Ultraviolet susceptibility, UV rate constants, D_{90} values, photodimerization, genomic modeling, pyrimidine dimers, viruses, ultraviolet germicidal irradiation, water disinfection, air disinfection, Z values, bioweapons, UVGI.

Introduction

The susceptibility of viruses to ultraviolet (UV) light has traditionally been defined in terms of the UV rate constant, also called a Z value, which is the slope of the survival curve on a logarithmic scale. The UV rate constant refers to either broad range UV in the UVB/UVC spectrum (200-320 nm) or, more commonly, to narrow-band UVC near the 253.7 nm wavelength. UV susceptibility can also be defined by the UV exposure dose (fluence) required for 90% inactivation (the D_{90} value) which is a more intuitive parameter that avoids the problem of shoulder effects and second stages in the decay curve. In this paper the UV rate constant is used in conjunction with a D_{90} value to provide an absolute indicator of UV susceptibility in the first stage of decay, and these values are thereby interchangeable. The UV rate constant, in m^2/J, applicable to the first stage of decay is defined as:

$$k = \frac{-\ln(S)}{D} \tag{1}$$

where S = survival, fractional
D = UV exposure dose (fluence), J/m^2

The D_{90} value associated with k is defined as:

$$D_{90} = \frac{-\ln(1-0.90)}{k} = \frac{-\ln(0.10)}{k} \tag{2}$$

UV rate constants and D_{90} values, as well as other terms defining UV susceptibility, have been determined in laboratory experiments and cataloged for decades, but as yet no one has produced a definitive theoretical model that can predict the ultraviolet susceptibility of microbes. The subject of virus UV susceptibility has been extensively studied and the processes that occur at the molecular level have been quantified to an extraordinary degree, but the complexities of these processes seem to have precluded development of a complete quantitative model of virus inactivation. The pieces to this complex puzzle have, in fact, been available in the literature for some time, particularly in the works of Setlow and Carrier (1966), Smith and Hanawalt (1969), Becker and Wang (1989), and others, but what was unavailable was specific knowledge about the genomes. Through the efforts and industry of molecular biologists, this gap has been filled over the previous two decades and a large number of viruses have had their genomes sequenced and published. This paper applies the basic inactivation models originally proposed by various researchers to an assortment of viral genomes from the NCBI database (NCBI 2009) and statistically evaluates the correlation with known UV D_{90} values. With some enhancements of the basic model and adjustments to the parameters, a new model is developed herein that provides fairly accurate predictions for both RNA and DNA viruses. This model

also includes a new ultraviolet scattering model developed by the authors that contributes to the overall accuracy of the DNA model.

Rate Constant Determinants

Various intrinsic factors determine the sensitivity of a virus to UV exposure under any set of constant ambient conditions of temperature and humidity. These include, but may not be limited to, the following species-dependent properties:

- Physical size
- Molecular weight of DNA or RNA
- DNA Conformation (A or B)
- Presence of chromophores or UV absorbers
- Propensity for clumping or agglutination
- Presence of repair enzymes or dark/light repair mechanisms
- Hydrophilic surface properties
- Relative Index of Refraction
- Specific UV spectrum (broad band UVC/UVB vs. narrow band UVC)
- G+C% and T+A%
- % of Potential Pyrimidine or Purine Dimers

The physical size of a virus bears no clear relationship with UV susceptibility, except that for the largest viruses, as size increases, the UV rate constant tends to decrease slightly (which is likely the result of UV scattering as discussed later). It might be expected that physical size would confer photoprotection through thickness alone, but it appears that the protein composition of the capsid, not its thickness, is a more important determinant due to the presence of UV-absorbing chromophores (Webb 1965).

Molecular weight has sometimes been cited as a factor in UV susceptibility (David 1973). However, it has been demonstrated that shearing DNA molecules to half size and then irradiating them does not alter the number of pyrimidine dimers or viral DNA inactivation, and this could be considered evidence that UV-induced damage to DNA is independent of molecular weight (Scholes et al 1967). Figure 1 illustrates this effect for a large number of viruses – there is no clear relationship between molecular weight (or genome size) and the D_{90} values for any of the virus types – double-stranded DNA, single-stranded RNA, double-stranded RNA, or single-stranded DNA.

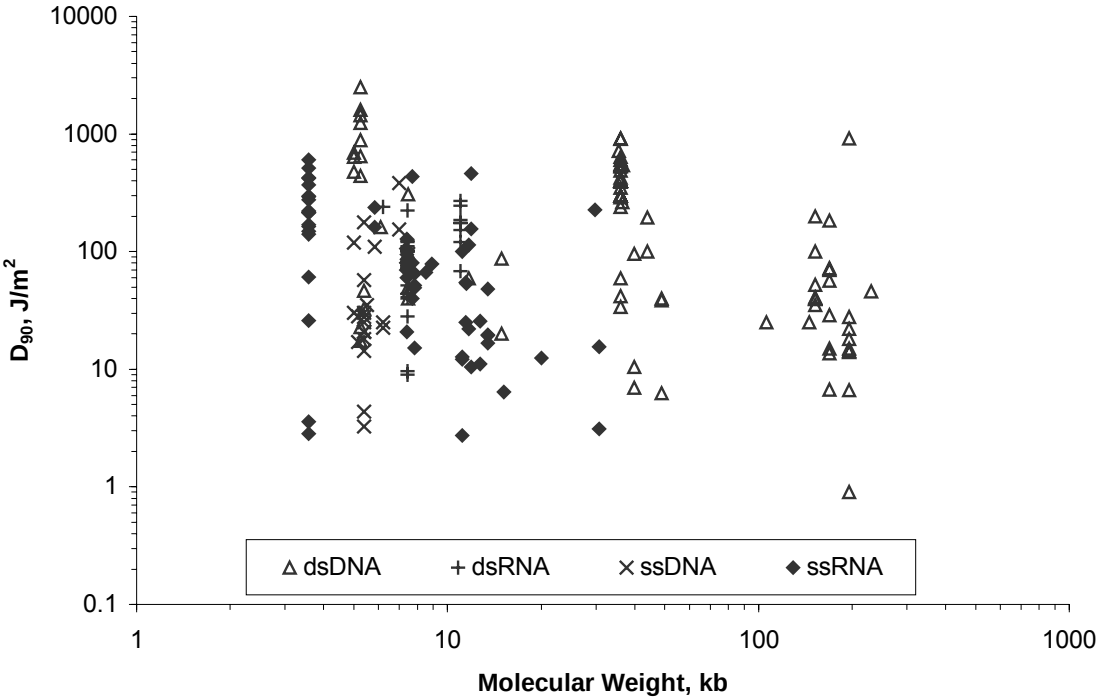

Figure 4.14: Plot of UV D_{90} vs. genome size for the four virus types.

Other suspected determinants can be dismissed because of their relatively minor or insignificant effect, such as the specific UV spectrum, the presence of repair enzymes, and hydrophilic surface properties. The DNA conformation is apparently a factor, but in this paper DNA viruses (in water – B conformation) are treated separately from RNA viruses (A-conformation). The matter of chromophore content and the relative index of refraction cannot be fully resolved at present and although they might be major factors, they are left for future research. Similarly, the propensity for clumping, which has been noted to be a protective factor, cannot be resolved due to a lack of detailed knowledge regarding chromophore content of envelopes and nucleocapsids.

One criteria worth examining in detail is the genomic G+C or T+A content. The genomic GC content of RNA viruses varies from about 30-60%, while that of DNA viruses varies from about 30-75%. One study on UVB irradiation of bacteria reports a strong correlation between the formation of cytosine-containing photoproducts with increasing GC content (Matallana-Surget 2008). Since an increased thymine content will likely result in a proportional increase in photodimers of the TT and CT variety, it could be expected that there must be some statistical relationship between G+C% (or conversely with T+A%) and UV susceptibility. Figure 2 shows the results of this comparison for 27 double-stranded DNA viruses and Figure 3 shows the same for 28 single-stranded DNA viruses irradiated in water. These comparison represent average UV rate constants for virus species where there are more than one data set. The DNA viruses show no significant correlation. The RNA viruses, however, show a fairly good correlation with an R^2 of about 45%. This latter result, however promising,

represents the limits of GC% content as a predictor of UV susceptibility, since it only provides an indicator of the presence of thymine doublets and triplets rather than an exact accounting of the potential dimers in any genome.

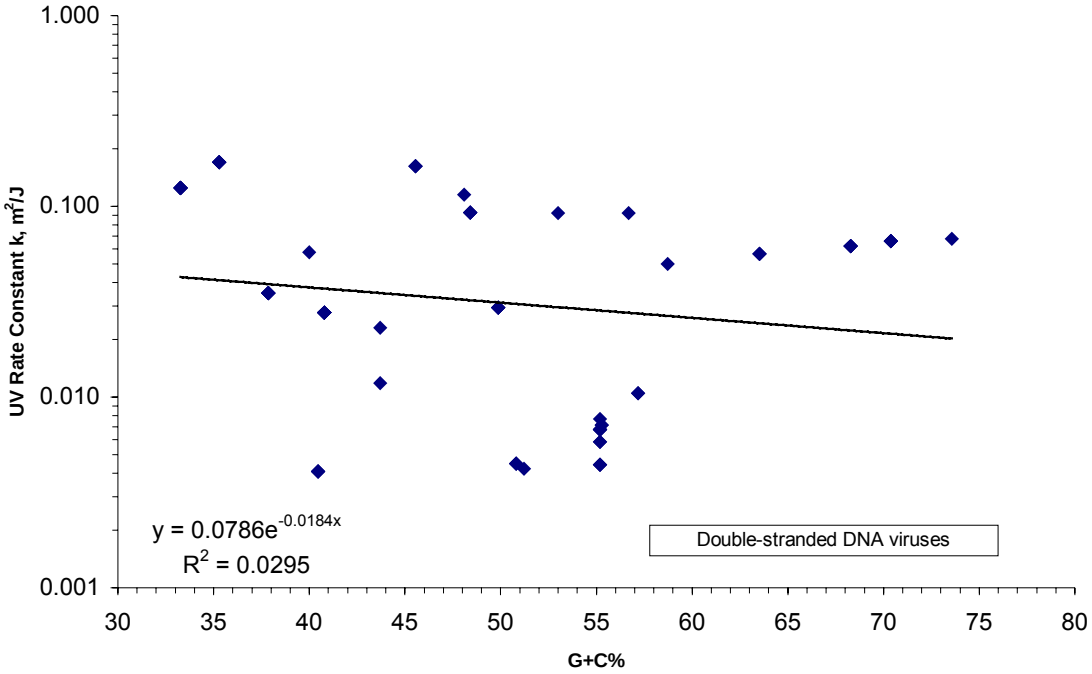

Figure 2: Plot of G+C% vs. UV rate constant for 27 dsDNA viruses, averaged per species. Line indicates exponential curve-fit with parameters as indicated.

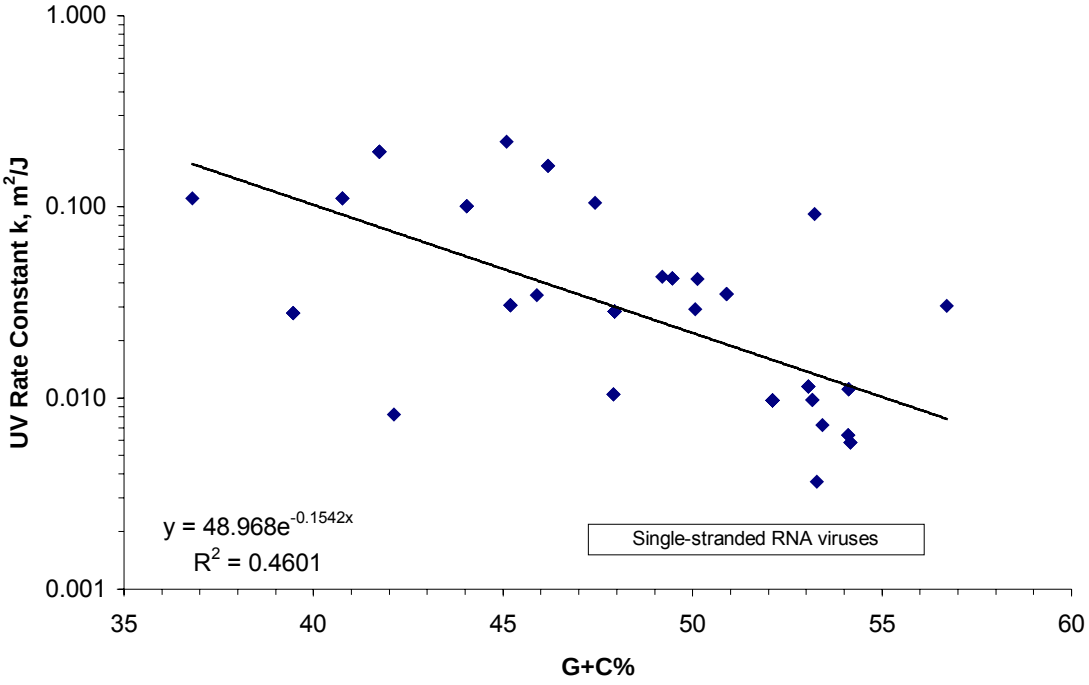

Figure 3: Plots of G+C% vs. UV susceptibility for 28 ssRNA viruses, averaged per species. Line indicates exponential curve-fit with parameters as indicated.

The UV Scattering Model

Viruses, which are about 0.02 microns and larger, are subject to ultraviolet scattering effects due to the fact that their size is very near the wavelength of ultraviolet light. The effect of scattering is to reduce the effective irradiance to which the microbe is exposed, and it is necessary to account for this attenuation before proceeding with the genomic model. The interaction between ultraviolet wavelengths and the particle is a function of the relative size of the particle compared with the wavelength, as defined by the size parameter:

$$x = \frac{2\pi a}{\lambda} \qquad (3)$$

where a = the effective radius of the particle
λ= wavelength

The scattering of light is due to differences in the refractive indices between the medium and the particle (Modest 1993, Garcia-Lopez et al 2006). The scattering properties of a spherical particle in any medium are defined by the complex index of refraction:

$$m = n - i\kappa \qquad (4)$$

where n = real refractive index
κ = imaginary refractive index (absorptive index or absorption coefficient)

The process of independent Mie scattering is also governed by the *relative refractive index*, defined as follows:

$$m = \frac{n_s}{n_m} \qquad (5)$$

where n_s = refractive index of the particle (a microbe)
n_m = refractive index of the medium (air or water)

The refractive index of microbes in visible light has been studied by several researchers. Balch et al (2000) found the median refractive index of four viruses to be 1.06, with a range of 1.03-1.26. Stramski and Kiefer (1991) assumed viruses to have a refractive index of 1.05. Biological cells were assumed by Mullaney and Dean (1970) to have *relative refractive indices* of about 1.05 in visible light. Klenin (1965) found *S. aureus* to have a refractive index in the range 1.05-1.12. Petukhov (1964) gives the refractive index of certain bacteria in the limits of 1.37-1.4. There are no studies that address the real refractive index of bacteria or viruses at UV wavelengths except Hoyle ans Wickramasinghe (1983) who suggest n_s = 1.43 as a reasonable choice for coliform bacteria. Water has a refractive index of n_m = 1.4 in the ultraviolet range. If we scaled the refractive index of viruses (Balch's value) to that of water (from visible to UV), the estimated real refractive index would be 1.06(1.4/1.33) = 1.12. Garcia-Lopez et al (2006) state that for soft-bodied biological particles n is between 1.04-1.45. All things considered, we choose n = n_s = 1.12 for the real refractive index of viruses under UV exposure. In fact, any value in the range 1.03-1.45 seems to have very little net impact on the fraction of scattered UV irradiation as was verified by multiple trials.

For the imaginary refractive index (the absorptive index) in the UV range no information is available. Per Garcia-Lopez et al (2006), hemoglobin has a κ of 0.01-0.15, while polystyrene has a κ of 0.01-0.82. However, we can reasonably assume a value comparable to that of water, k=1.4, or any value in the range of the real refractive indices given above as they have even less overall impact than the choice of the real refractive index. These values were used as input to a Mie Scattering program (Prahl 2009) to estimate the effects of UV scattering at the wavelength of 253.7 nm, and with negligible concentrations (0.000001 spheres/μm^3).

Table 1 below summarizes the primary parameters computed by the Mie Scattering program in the first eight columns (Prahl 2001), including the scattering efficiency (Q_{sca}), the extinction efficiency (Q_{ext}), the absorption efficiency (Q_{abs}), the scattering cross-section (C_{sca}), the extinction cross-section (C_{ext}), and the absorption cross-section (C_{abs}). The efficiency terms are essentially self-defining but readers may consult the references for detailed definitions and further information on Mie theory (Modest 1993, vandeHulst 1957,

Bohren and Huffman 1983). The scattering cross-section represents the area which when multiplied by the incident irradiance gives the power scattered by the particle. The extinction cross-section represents the area which when multiplied by the incident irradiance gives the total power removed from the incident wave by scattering and absorption. The final column shows the computed ratio of the scattering cross-section to the extinction cross-section, which represents the fraction of total irradiance that is scattered away. This fraction is used to reduce the UV exposure dose for the microbes in the genomic model.

Table 1: Mie Scattering Parameters for UV in Water

Diameter μm	Size Para x	Q_{sca}	Q_{ext}	Q_{abs}	C_{sca} μm^2	C_{ext} μm^2	C_{abs} μm^2	C_{sca}/C_{ext} (UV scatter)
0.01	0.17336	0.0020	0.6328	0.630759	1.56E-07	0.000050	0.00005	0.00
0.02	0.34673	0.02950	1.236	1.206502	9.27E-06	0.000388	0.0004	0.02
0.03	0.52009	0.12498	1.7312	1.60622	0.000088	0.00122	0.0011	0.07
0.04	0.69345	0.29531	2.0564	1.76109	0.000371	0.00258	0.0022	0.14
0.05	0.86682	0.4937	2.237	1.7433	0.000969	0.00439	0.0034	0.22
0.06	1.0402	0.6704	2.3456	1.6753	0.001895	0.00663	0.0047	0.29
0.07	1.2135	0.8089	2.431	1.6221	0.0031	0.0094	0.0062	0.33
0.08	1.3869	0.9173	2.5039	1.5866	0.0046	0.0126	0.0080	0.37
0.09	1.5603	1.0074	2.5585	1.5511	0.0064	0.0163	0.0099	0.39
0.1	1.7336	1.0841	2.5938	1.5097	0.0085	0.0204	0.0119	0.42
0.12	2.0804	1.2005	2.6316	1.4311	0.0136	0.0298	0.0162	0.46
0.15	2.6004	1.3103	2.6499	1.3396	0.0232	0.0468	0.0237	0.49
0.2	3.4673	1.4048	2.6283	1.2235	0.0441	0.0826	0.0384	0.53
0.3	5.2009	1.4695	2.5501	1.0806	0.1039	0.1803	0.0764	0.58
0.4	6.9345	1.4855	2.4824	0.9969	0.1867	0.3120	0.1253	0.60
0.5	8.6682	1.4881	2.4298	0.9417	0.2922	0.4771	0.1849	0.61
0.8	13.869	1.4782	2.3289	0.8507	0.7430	1.1706	0.4276	0.63
0.9	15.603	1.4738	2.3064	0.8326	0.9376	1.4673	0.5297	0.64
1	17.336	1.4697	2.2873	0.8176	1.1543	1.7964	0.6421	0.64
2	34.673	1.4392	2.1854	0.7462	4.5214	6.8656	2.3442	0.66
4	69.345	1.411	2.1179	0.7069	17.731	26.614	8.8830	0.67

Figure 4 illustrates three parameters from Table 1, the scattering efficiency, the absorption efficiency, and the scattered fraction of incident UV irradiance. The reason that the efficiencies exceed a value of unity is due to the extinction paradox – the fact that in this size range more light can be intercepted than would be by the size of the spherical particle alone. It can be observed that the scattering efficiency increases sharply through the DNA virus size range while the absorption efficiency peaks and then decreases. It can also be seen that the fraction of scattered UV is relatively minor for most RNA viruses, but increases sharply through the DNA virus size range, approaching a limit of about 0.68. The values for UV scatter, last column in Table 1, are hereafter used to decrease the incident UV irradiance (in effect decreasing the UV dose), and may be thought of as correction factors.

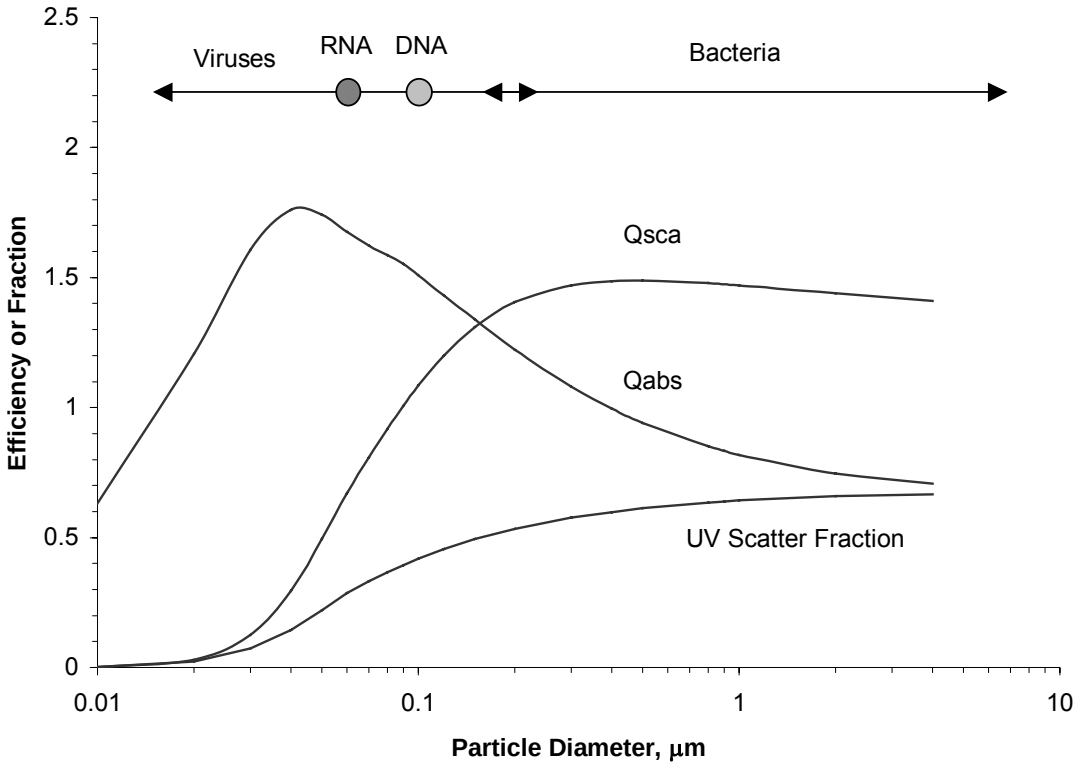

Figure 4: Plot of scattering efficiency (Qsca), absorption efficiency (Qabs), and the fraction of incident UV scattered away.

Table 2 shows the diameters of the viruses used in this study and the associated UV scatter correction factors, (which are later applied to the raw D_{90} values shown in Tables 3 and 4). Virus diameters were obtained from various sources (i.e. Kowalski 2006) and some online databases. Diameters are generally logmean values of the smallest dimension or logmean values of ovoid envelopes, since the logmean value always represents the natural distribution when multiple sizes or a range of sizes occurs. It should be noted that for larger viruses that have an envelope, secondary UV scattering effects may also occur in the nucleocapsid, but these effects are ignored in the current model.

Table 2: Virus Mean Diameters and UV Scattering Corrections

Virus	Type	Diameter μm	UV Scatter Correction	Virus	Type	Diameter μm	UV Scatter Correction
Bacteriophage MS2	DNA	0.020	0.9732	B. subtilis phage SP	DNA	0.087	0.6122
Echovirus (Parechovirus)	RNA	0.024	0.9552	Coliphage T4	DNA	0.089	0.6057
Encephalomyocarditis virus	RNA	0.025	0.9501	Borna virus	DNA	0.090	0.6026
Coxsackievirus	RNA	0.027	0.9391	Friend Murine Leukemia virus	DNA	0.094	0.5907
Hepatitis A virus	RNA	0.027	0.9391	Moloney Murine Leukemia virus	RNA	0.094	0.5907
Murine Norovirus	RNA	0.032	0.9086	Rauscher Murine Leukemia virus	RNA	0.094	0.5907
Feline Calicivirus (FCV)	DNA	0.034	0.8955	Avian Sarcoma virus	RNA	0.098	0.5798
Canine Calicivirus	RNA	0.037	0.8755	Influenza A virus	RNA	0.098	0.5798
Polyomavirus	RNA	0.042	0.8389	BLV	DNA	0.099	0.5772
Simian virus 40	RNA	0.045	0.8214	Murine Cytomegalovirus	RNA	0.104	0.5649
Coliphage lambda	RNA	0.050	0.7889	Vesicular Stomatitis virus (VSV)	RNA	0.104	0.5649
Coliphage T1	DNA	0.050	0.7889	Equine Herpes virus	RNA	0.105	0.5626
Semliki Forest virus	DNA	0.061	0.7240	Avian Leukosis virus	RNA	0.107	0.5581
Coliphage PRD1	DNA	0.062	0.7186	Coronavirus (incl SARS)	RNA	0.113	0.5457
HP1c1 phage	DNA	0.062	0.7186	Murine sarcoma virus	RNA	0.120	0.5330
Coliphage T7	DNA	0.063	0.7133	HIV-1	RNA	0.125	0.5249
Mycobacterium phage D29	DNA	0.065	0.7030	Rous Sarcoma virus (RSV)	DNA	0.127	0.5218
VEE	DNA	0.065	0.7030	Frog virus 3	RNA	0.167	0.4793
Adenovirus Type 40	RNA	0.069	0.6835	Herpes simplex virus Type 2	RNA	0.173	0.4750
Rabies virus	RNA	0.070	0.6788	Herpes simplex virus Type 1	RNA	0.184	0.4681
WEE	DNA	0.070	0.6788	Pseudorabies (PRV)	DNA	0.194	0.4626
Sindbis virus	DNA	0.075	0.6569	Newcastle Disease Virus	DNA	0.212	0.4544
Adenovirus Type 1	RNA	0.079	0.6408	Vaccinia virus	DNA	0.307	0.4280
Adenovirus Type 2	RNA	0.079	0.6408	Measles	DNA	0.329	0.4237
Adenovirus Type 5	DNA	0.084	0.6224	*NOTE: Virus diameters represent logmean values.*			

The Genomic UV Susceptibility Model

Double stranded DNA viruses are likely to be the most resistant to UV than single stranded viruses and therefore separate models for ssRNA and dsDNA are appropriate (Gerba et al (2002). Van der Eb and Cohen (1967) demonstrated that the double stranded version of Polyoma virus DNA was four times more resistant to UV inactivation. Capsid structure, as well as nucleic acid size, render double-stranded DNA less susceptible to UV inactivation (Thurston-Enriquez et al 2003). Based on an extensive review of UV rate constants (data not shown), this does appear to be the case, with dsDNA and dsRNA viruses having almost half the UV rate constant of ssRNA and ssDNA viruses.

The disruption of normal DNA processes occurs as the result of the formation of photodimers, but not all photoproducts appear with the same frequency. Purines are approximately ten times more resistant to photoreaction than pyrimidines (Smith and Hanawalt 1969). Minor products other than CPD dimers, such as interstrand cross-links, chain breaks, and DNA-protein links occur with much less frequency, typically less than 1/1000 of the number of cyclobutane dimers and hydrates may occur at about 1/10 the frequency of cyclobutane dimers (Setlow 1966). Although irradiated vegetating cells produce large amounts of cyclobutane pyrimidine dimers, thymine-containing photoproducts isolated from bacterial spores do not include cyclobutane pyrimidine dimers but include spore photoproducts. Spore photoproducts decrease when the spore transforms to a vegetative state and thymine dimers increase. Spore photoproducts also appear in dry DNA (A conformation) and in RNA, which is in permanent A conformation. For DNA, the thymine dimers decrease under dry conditions (A-DNA) and the spore photoproduct is formed

and can become the dominant photoproduct (Rahn and Hosszu 1969). The rate of spore photoproduct formation is unaffected by high concentrations of thymine dimers but high concentrations of spore photoproduct inhibit dimer formation.

Wang (1964) first suggested that dimerization is favored when adjacent pyrimidine triplets in ice are suitably oriented and positioned. The effect of base composition can impact the intrinsic sensitivity of DNA to UV irradiation (Smith and Hanwalt 1969). The specific sequence of adjacent base pairs, as well as the frequency of thymines, can de determinants of UV sensitivity. Setlow and Carrier (1966) stated that the probability of photodimerization is approximately proportionally to the nearest-neighbor frequencies of the various pyrimidine sequences. Some 80% of pyrimidines and 45% or purines form UV photoproducts in double-stranded DNA, per studies by Becker and Wang (1989), who also showed that purines only form dimers when adjacent to a pyrimidine doublet. The formation of purine dimers requires transfer of energy in neighboring pyrimidines, and will only occur on the 5' side of the purine base (50% probability). Becker and Wang (1985) formulated these simple rules for sequence-dependent DNA photoreactivity:

1. Whenever two or more pyrimidine residues are adjacent to one another, photoreactions are observed at both pyrimidines.
2. Non-adjacent pyrimidines, surrounded on both sides by purines, exhibit little or no photoreactivity.
3. The only purines that readily form UV photoproducts are those that are flanked on their 5' side by two or more contiguous pyrimidine residues.

These rules can be used to extract information from DNA and RNA genomes and will enable computation of the relative probability of photoreactions taking place, a parameter that can be directly compared to UV rate constants as a possible predictor. Table 1 summarizes these rules in terms that can be computed numerically. The doublets and triplets in Table 3 were counted using base counting software written by the author (in C++) and reading from genomes obtained from NCBI (2009). Similar base-counting programs (wordcount programs) are publicly available, such as EMBOSS (Rice et al 2000).

Table 3: Potential Dimerization Sequences

Group	DNA Sequence				Dimer
Adjacent pyrimidines	TT	TC	CT	CC	Yes
Purines flanked by doublets	ATT	ACC	ACT	ATC	50% Yes
	GTT	GCC	GCT	GTC	50% Yes
	TTA	CCA	CTA	TCA	50% Yes
	TTG	CCG	CTG	CGT	50% Yes
Surrounded pyrimidines	ATA	ATG	GTA	GTG	No
	ACA	ACG	GCA	GCG	No

Ignoring the other factors that may determine the UV rate constant, such as the protein coat in viruses and the cell walls of bacteria, about which not

enough is known, a function can be written to sum the dimerization probabilities. The probability density map of a spherical genome can be represented by a circular cross-section of the sphere which is subject to a collimated beam of irradiance. The volume of the sphere will be directly proportional to the genome size, since the nucleic acids are essentially packed tight inside a capsid, and because almost all animal viruses of interest are spherical, ovoid, or possess a spherical capsid atop a tail. The size of the model sphere is directly proportional to the base pairs (bp) of the genome cubed, and the area of the cross-section is then the square root of the cube of the base pairs, as illustrated in Figure 4. The dimerization probabilities can be viewed as collapsed onto a circular cross-section exposed to a collimated beam of UV rays. The probability map is illustrative purposes only – the square root of the total dimer probabilities is assumed to be distributed evenly across the cross-sectional area in this model.

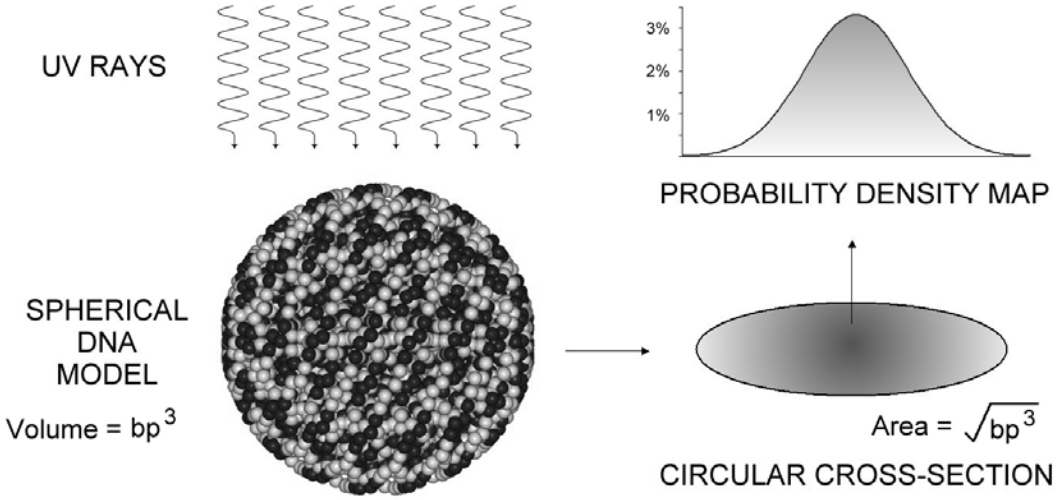

Figure 4: The spherical model of DNA has a circular cross-section with a collapsed dimerization probability density map subject to collimated UV rays.

The square root of the dimer probabilities, counted as per Table 1, is used because it was found on analysis that this produces the best fit overall (for both RNA and DNA), and so without further theoretical justification the dimerization probability equation for ssRNA viruses is written:

$$D_v = \frac{\left[\sum tt + F_a \sum \overleftrightarrow{ct} + F_b \sum cc + F_c \sum \overleftrightarrow{YYU}\right]^{0.5}}{\sqrt[3]{bp^2}} \qquad (6)$$

where D_v = dimerization probability value
tt = thymine doublets
cc = cytosine doublets
$\overleftrightarrow{ct}$ = ct and tc (counted both ways, exclusive)

$\overleftrightarrow{YYU}$ = purine w/ adjacent pyrimidine doublet (counted both ways, exclusive)

bp = total base pairs

F_a, F_b, F_c = dimer proportionality constants

Some evidence is available in the literature to allow some starting estimates of the dimer proportionality constants. Per Setlow and Carrier (1966) the average for three bacteria is 1:0.25:0.13. Patrick (1977) suggests ratios of 1:1:1. Unrau (1973) found the ratio was 1:0.5:0.5. Meistrich et al (1970) indicate that in *E. coli* DNA, the proportions of TT dimers, CT dimers, and CC dimers are in the ratio 1:0.8:0.2, as did Lamola (1973). Table 4 lists 62 of the 70 virus data sets that were used in the ssRNA model, along with the average rate constants and the average D_{90} values representing 27 single-stranded RNA viruses. These D_{90} values are not adjusted for UV scatter (per the Table 2 correction factors).

Table 4: Rate Constants and D_{90} Values for RNA Viruses

Virus	NCBI ID#	Genome bp	D_{90} J/m^2	UVGI k m^2/J	Avg k m^2/J	Avg D_{90} J/m^2	Source
Bacteriophage MS2*	NC_001699	3569	295	0.00780	0.01	237	Ko 2005
		3569	275	0.00837			Thurston-Enriquez 2003
		3569	250	0.00920			Battiggelli 1993
		3569	217	0.01060			Simonet 2006
		3569	217	0.01063			deRodaHusman 2004
		3569	213	0.01080			Butkus 2004
		3569	187	0.01230			Oppenheimer 1997
Murine sarcoma virus	NC_001502	5833	237	0.0097	0.0111	207	Nomura 1972
		5833	144	0.016			Kelloff 1970
		5833	299	0.0077			Yoshikura 1971
Coxsackievirus	NC_001612	7413	128	0.02	0.02834	81	Hill 1970
		7413	86	0.026837			Havelaar 1987
		7413	80	0.02878			Gerba 2002
		7413	60	0.03840			Shin 2005
		7413	95	0.02424			Gerba 2002
		7413	72	0.03180			Battigelli 1993
Echovirus	NC_001897	7345	106	0.02190	0.027859	83	Hill 1970
		7345	80	0.02878			Gerba 2002 (type 1)
		7345	70	0.03289			Gerba 2002 (type 2)
Feline Calicivirus (FCV)	NC_001699	7677	434	0.0053	0.030567	75	Nuanualsuw an 2002
		7677	80	0.0288			Thurston-Enriquez 2003
		7677	40	0.0576			deRodaHusman 2004
Canine Calicivirus	NC_004542	8513	67	0.0345	0.0345	67	deRodaHusman 2004
Encephalomyocarditis virus	NC_001479	7835	50	0.0465	0.0422	55	Ross 1971
		7835	52	0.0446			Rauth 1965
		7835	65	0.0355			Zavadova 1968
Influenza A virus	NC_007366-73	13498	20	0.117	0.10103	23	Ross 1971
		13498	48	0.048			Hollaender 1944
		13498	17	0.1381			Abraham 1979
Vesicular Stomatitis virus (VSV)	NC_001560	11161	13	0.1806	0.1944	12	Rauth 1965
		11161	12	0.19			Helentjaris 1977
		11161	100	0.023			Bay 1979
		11161	6	0.384			Shimizu 2004
Newcastle Disease Virus	NC_002617	15186	8	0.276	0.1636	14	vonBrodorotti 1982
		15186	45	0.0511			Levinson 1966
Borna virus	NC_001607	8910	79	0.0292	0.0292	79	Danner 1979
Rabies virus	NC_001542	11932	10	0.2193	0.2193	10	Weiss 1986
Rauscher Murine Leukemia virus	NC_001819	8282	157	0.0147	0.00975	236	Kelloff 1970
		8282	480	0.0048			Lovinger 1975
Coronavirus (incl SARS)	NC_005147	30738	7	0.321	0.1106	21	Weiss 1986
	NC_004718	29751	226	0.01			Kariw a 2004
	NC_004718	29751	3046	0.000756			Darnell 2004
VEE	NC_001449	11438	55	0.04190	0.04190	55	Smirnov 1992
Avian Sarcoma virus	NC_008094	3166	155	0.0149	0.01047	220	Ow ada 1976
		3166	381	0.00604			Bister 1977
WEE	NC_003908	11484	54	0.043	0.04300	54	Dubinin 1975
Rous Sarcoma virus (RSV)	NC_001407	9392	720	0.0032	0.00640	360	Levinson 1966
		9392	240	0.0096			Golde 1961
Murine Norovirus	NC_008311	7382	76	0.0304	0.03040	76	Lee 2008
Semliki Forest virus	NC_003215	11442	25	0.0921	0.09210	25	Weiss 1986
Sindbis virus	NC_001547	11703	60	0.038645	0.03501	66	vonBrodorotti 1982
		11703	113	0.0203			Wang 2004
		11703	50	0.0461			Zavadova 1975
BLV	NC_001414	8419	1799	0.00128	0.00584	394	Shimizu 2004
		8419	221	0.01040			Guillemain 1981
HIV-1	NC_001802	9181	280	0.00822	0.00822	280	Yoshikura 1989
Avian Leukosis virus	NC_001408	7286	631	0.00365	0.00365	631	Levinson 1966
Measles	NC_001498	15894	22	0.10510	0.10510	22	DiStefano 1976
Moloney Murine Leukemia virus	NC_001501	8332	115	0.02	0.01148	201	Nomura 1972
		8332	370	0.00622			Guillemain 1981
		8332	280	0.00822			Yoshikura 1989
Friend Murine Leukemia virus	NC_001362	8323	320	0.0072	0.00720	320	Yoshikura 1971

Figure 5 shows a plot of equation (3) applied to ssRNA viruses that were averaged per species where more than one data set was available. The D_{90} value is plotted versus the dimerization probability value for clarity -- identical results are obtained if the rate constant is plotted instead. Only water-based test results were used since they are the most numerous and they all represent the B-DNA conformation. Data was culled exclusively from the literature and no animal virus or bacteriophage was omitted from consideration, although a few redundant studies could not be obtained. The data sets for MS2 (marked with an asterisk in Table 4), however, were so numerous that although they were all averaged, only seven data points were credited, so as not to give undue weight to this particular phage. The remaining eight data sets for MS2 are listed in the References (Furuse and Watanabe 1971, Sommer et al 2001, Mamane-Gravetz et al 2005, Templeton et al 2006, Nuanualsuwan 2002, Rauth 1965, Shin et al 2005, Meng and Gerba 1996). Only one anomalous outlier was excluded from the 70 data sets -- HTLV-1: Human T-cell Leukemia virus (Shimizu et al 2004), which was unusually distant from the other data points for reasons yet unknown. There is a fairly definitive relationship across the entire potential dimerization range. The dimer proportionality constants used to fit equation (3) were: 1:0.1:6:6 (with the fourth constant being 4 for the triplets), or F_A=0.1, F_B=6, F_C=6.

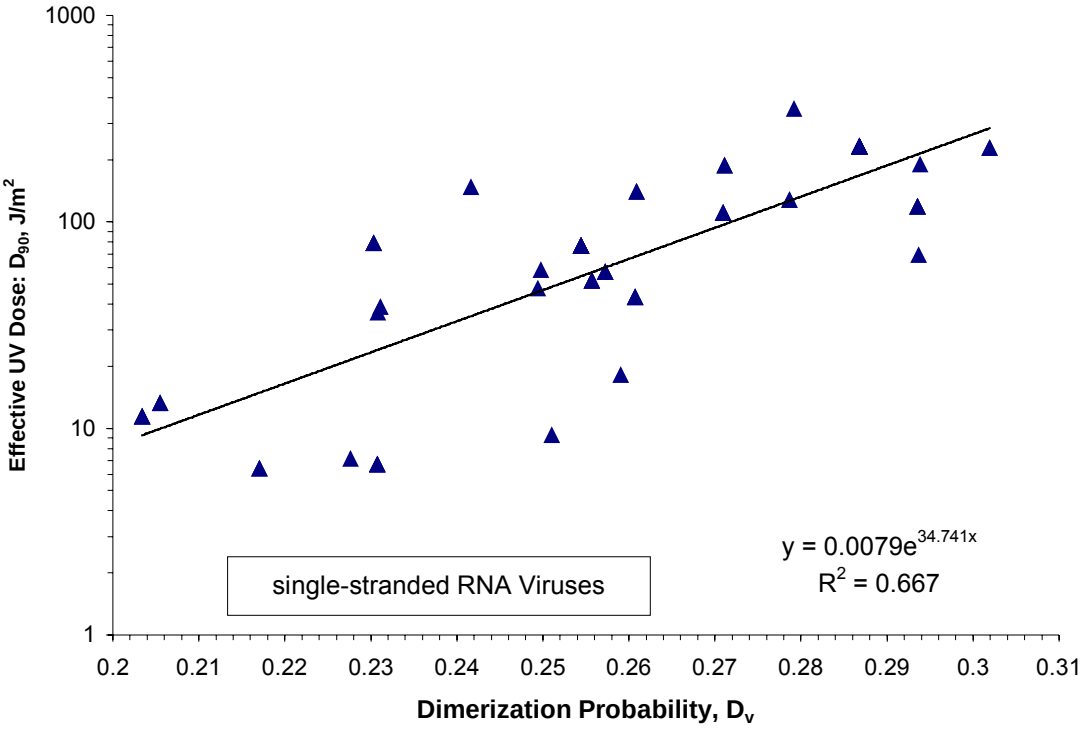

Figure 5: Plot of D_v versus effective D_{90} values for RNA animal viruses and bacteriophages – D_{90} is the effective dose because of correction for scatter. The line represents a curve fit (equation shown on graph), fit to 27 viruses, representing 70 data sets for UV irradiation tests in water.

Insufficient data was available to adequately model single-stranded DNA viruses separately, and they appeared sufficiently different from ssRNA viruses that they were not modeled together (likewise for double stranded RNA viruses in the dsDNA model). Application of the ssRNA model to dsDNA viruses requires some modifications. DNA is double stranded, with a 'template' strand and a complementary strand. The template strand will be accounted for in equation (6) but the complementary strand is not. However, a TT doublet in the complementary strand will be represented by an AA doublet on the template strand, and so counting base pairs can be done with the template strand alone, by converting them to their complementary bases. Incorporating the complementary strand bases produces the following equation:

$$D_v = \frac{\left[\sum(tt+aa) + F_a\sum(\overleftrightarrow{ct}+\overleftrightarrow{ag}) + F_b\sum(cc+gg) + F_c\sum\left(\overleftrightarrow{YYU}+\overleftrightarrow{UUY}\right)\right]^{0.5}}{\sqrt[3]{bp^2}} \qquad (7)$$

where $\overleftrightarrow{ct}$ = ct and tc (both ways, exclusive)
$\overleftrightarrow{ag}$ = ag and ga (both ways, exclusive)
$\overleftrightarrow{YYU}$ = YYU and UYY (both ways, exclusive)
$\overleftrightarrow{UYY}$ = UUY and YUU (both ways, exclusive)
F_a, F_b, F_c = proportionality constants

In addition to the doublets and triplets, it was found that the quadruplets onwards also contributed to the model (which they did not for RNA viruses). The effect of the quadruplets, quintuplets, sextuplets, septuplets, and octuplets onwards can be characterized by a factor that accounts for hyperchromicity. Hyperchromicity occurs when the absorbance of a given oligonucleotide is higher than its constituents molecules. Hyperchromicity is largely explained by the coulombic interaction of the ordered bases in the polymer, and is a kind of resonant electronic effect in which the partial alignment of transition moments by base stacking results in coupled oscillation. Hyperchromicity is analogous to the way photosensitive sunglasses darken under sunlight, thereby absorbing more solar radiation. Hyperchromicity occurs when multiple pyrimidines, especially thymines, are stacked sequentially in clusters of three or more with the effect leveling off at about 8-10 pyrimidines in a row. A relatively small number of bases in a DNA strand are required for such coupling and about 8-10 base pairs can exhibit roughly 80% of the hyperchromism of an infinite helix. The effect appears to increase the probability of photodimerization by a factor of about 2 with 8 or more bases in a row, based on the data from Becker and Wang (1989).

Although not enough is known about the hyperchromic effect to quantify it exactly, a factor can be added to equation (7) to increase the probability of dimerization of any doublet or triplet whenever 3 or more pyrimidines are found in sequence. Since isolated doublets and triplets are already addressed their hyperchromicity factor can be assumed equal to 1. The value of the factor can then be estimated by curve-fitting the data to obtain the best fit. In the present

model the factor linearly increases the probability of dimerization for doublets and triplets based on how many adjacent pyrimidines are present in the genome, up to a value of 8 in a row. Each contribution can be defined as follows:

tt_n = # of tt doublets within n pyrimidines (template strand)
aa_n = # of aa doublets within n purines (complement strand)
tc_n = # of tc doublets within n pyrimidines (template strand)
ag_n =# of ag doublets within n purines (complement strand)
cc_n =# of cc doublets within n pyrimidines (template strand)
gg_n =# of gg doublets within n purines (complement strand)
UYY_n =# of UYY triplets within n pyrimidines (template strand)
UUY_n =# of UUY triplets within n purines (complement strand)

All the triplets above are counted exclusively – once one doublet or triplet is located in the genome, it is excluded from participating in other dimers. There is a slight problem with sequence in this algorithm – once a specific doublet is searched for and found it may exclude other doublets or triplets of greater value as potential photodimers. The same is true for all the doublets and triplets that are counted, but it is assumed the effect, if any, is negligible.

The equations for assigning the increase in probability due to hyperchromicity can then be written as follows:

$$tt_h = H\sum_{n=3}^{8}\left(n \cdot tt_n\right) \quad (8)$$

$$aa_h = H\sum_{n=3}^{8}\left(n \cdot aa_n\right) \quad (9)$$

$$tc_h = H\sum_{n=3}^{8}\left(n \cdot tc_n\right) \quad (10)$$

$$ag_h = H\sum_{n=3}^{8}\left(n \cdot ag_n\right) \quad (11)$$

$$cc_h = H\sum_{n=3}^{8}\left(n \cdot cc_n\right) \quad (12)$$

$$gg_h = H\sum_{n=3}^{8}\left(n \cdot gg_n\right) \quad (13)$$

$$UYY_h = H\sum_{n=3}^{8}\left(n \cdot UYY_n\right) \quad (14)$$

$$UUY_h = H\sum_{n=3}^{8}\left(n \cdot UUY_n\right) \quad (15)$$

where tt_h = hyperchromic multiplier, or increase in probability of dimerization from all multiple sequences of 3 to 8 pyrimidines. Similar for all other hyperchromic constants aah, tch, agh, cch, ggh, UYYh, and UUYh.

In equations (8) through (15), hyperchromic regions above 8 are neglected since such extended regions tend to be rare, and will be partly accounted for by these factors (i.e. any region of 8 pyrimidines in a row will contain a region of 8 in a row). The hyperchromicity model presented above is a crude linear approximation and although it works for DNA viruses, it remains an area for future research. More complex logarithmically increasing hyperchromicity models did not work as well as this simple one. Equation (5) is therefore re-written as follows:

$$D_v = \frac{\left[\begin{array}{c} \sum\left(tt + aa + tt_h + aa_h\right) + F_a \sum\left(\overleftrightarrow{ct} + \overleftrightarrow{ag} + \overleftrightarrow{ct}_h + \overleftrightarrow{ag}_h\right) + \\ F_b \sum\left(cc + gg + cc_h + gg_h\right) + F_c \sum\left(\overleftrightarrow{YYU} + \overleftrightarrow{UUY} + \overleftrightarrow{YYU}_h + \overleftrightarrow{UUY}_h\right) \end{array}\right]^{0.5}}{\sqrt[3]{bp^2}} \quad (16)$$

The proportionality constants represent the relative proportions of each type of dimer, which differ in RNA and DNA. Applying this model to DNA viruses produces the result shown in Figure 6. The dimer ratios for this curve fit were 1:0.2:40:18 (F_A=0.2, F_B=40, F_C=18), with a hyperchromicity factor H = 0.67. It should be noted that since the hyperchromicity factor adds on to the existing doublets and triplets it is the same as multiplying them by a factor of 1.67, which is reasonably close to the factor of 2 estimated previously. Even though DNA viruses tend to be larger and likely have more protective mechanisms (i.e. protein coats), the pattern of increasing D_{90} with increasing values of D_v seems fairly definitive. Table 5 lists 67 of the 77 virus data sets that were used in the ssRNA model, along with the average rate constants and the average D_{90} values representing 27 single-stranded RNA viruses. Viruses marked with an asterisk (*) indicate that additional data sets were used to compute the average rate constants – a maximum of 7 data sets were used per virus so as not to give undue weight to any virus. The remaining data sets are given in the References (Rainbow and Mak 1973 & 1970, Linden et al 2007, Wang et al 2004, Bossart et al 1978, Bourre et al 1989). In addition, two data sets for T7 (MP and LP values) were accounted for in Table 5 (k=0.056 m^2/J and k=0.061 m^2/J) but not listed (Bohrerova et al 2008). The D_{90} values in Table 5 are uncorrected for UV scatter.

Table 5: Rate Constants and D_{90} Values for DNA Viruses

Virus	NCBI ID#	Genome bp	D_{90} J/m^2	UVGI k m^2/J	Avg k m^2/J	Avg D_{90} J/m^2	Source
Adenovirus Type 1	AC_000017	35997	299	0.0077	0.00714	322	Battiggelli 1993
			350	0.0066			Nwachuku 2005
Adenovirus Type 2*	AC_000007	35937	300	0.0077	0.00691	333	Shin 2005
			400	0.0058			Gerba 2002
Adenovirus Type 5*	AC_000008	35938	400	0.0058	0.00441	522	Durance 2005
			720	0.0032			Nwachuku 2005
Adenovirus Type 40	NC_001454	34214	546	0.0042	0.00422	546	Thurston-Enriquez 2003
Coliphage lambda	NC_001416	48502	57	0.0405	0.02953	78	Gurzadyan 1981
			70	0.0331			Harm 1961
			72	0.0320			Weigle 1953
			184	0.0125			Davidovich 1991
Simian virus 40*	NC_001669	5243	1599	0.0014	0.02768	83	Seemayer 1973
			1439	0.0016			Cornellis 1981
			1245	0.0019			Bockstahler 1977
			886	0.0026			Defendi 1967
			650	0.0035			Sarasin 1978
			443	0.0052			Aaronson 1970
			23	0.1004			Cornellis 1982
Hepatitis A virus	NC_001489	7478	40	0.0576	0.03513	66	Battigelli 1993
			45	0.0512			Wang 2004
			50	0.0461			Wiedenmann 1993
			92	0.0250			Wang 1995
			98	0.0234			Wilson 1992
			307	0.0075			Nuanualsuwan 2002
Herpes simplex virus Type 1	NC_001806	152261	100	0.0230	0.06262	37	Bockstahler 1976
			110	0.0209			Selsky 1978
			25	0.0933			Lytle 1971
			35	0.0654			Ross 1971
			21	0.1105			Albrecht 1974
Coliphage PRD1	NC_001421	14925	20	0.1150	0.115	20	Shin 2005
Vaccinia virus*	NC_006998	198350	7	0.3490	0.12454	18	Galasso 1965
			14	0.1604			Ross 1971
			18	0.1279			Klein 1994
			22	0.1050			Zavadova 1971
			28	0.0829			Rauth 1965
			715	0.0032			Davidovich 1991
			677	0.0034			Collier 1955
Coliphage T4	NC_000866	168900	7	0.3450	0.1709	13	Otaki 2003
			14	0.1685			Ross 1971
			15	0.1540			Harm 1968
			29	0.0800			Templeton 2006
			22	0.1070			Winkler 1962
B. subtilis phage SP	NC_004166	44010	100	0.0230	0.01742	132	Freeman 1987
			195	0.0118			Freeman 1987
Pseudorabies (PRV)	NC_005946	143461	34	0.0676	0.0676	34	Ross 1971
Murine Cytomegalovirus	NC_004065	230278	46	0.0500	0.05	46	Shanley 1982
HP1c1 phage	NC_001697	32355	40	0.0576	0.0576	40	Setlow 1972
Equine Herpes virus	NC_005946	150224	25	0.0921	0.0921	25	Weiss 1986
Frog virus 3	NC_005946	105903	25	0.0921	0.0921	25	Martin 1982
Coliphage T1	NC_005833	48836	6	0.3697	0.163	14	Hotz 1969
			38	0.0600			Harm 1968
			40	0.0580			Fluke 1949 (265 nm)
Coliphage T7	NC_001604	39937	95	0.0242	0.08192	25	Benzer 1952
			23	0.1000			Ronto 1992
			53	0.0432			Peak 1978 (B)
			11	0.2047			Peak 1978 (Bs-1)
Polyomavirus	NC_001699	5130	480	0.0048	0.0071	324	vander Eb 1967
			640	0.0036			Defendi 1967
			696	0.0033			Rauth 1965
			501	0.0046			Latarjet 1967
Mycobacterium phage D29	NC_001348	49136	16	0.1430	0.05623	41	David 1973
			324	0.0071			Sellers 1970 (D29)
			268	0.0086			Sellers 1970 (D29A)
Herpes simplex virus Type 2	NC_001798	154746	40	0.0576	0.06569	35	Wolff 1973
			41	0.0565			Ross 1971
			75	0.0307			Ryan 1986
			20	0.1180			Albrecht 1974

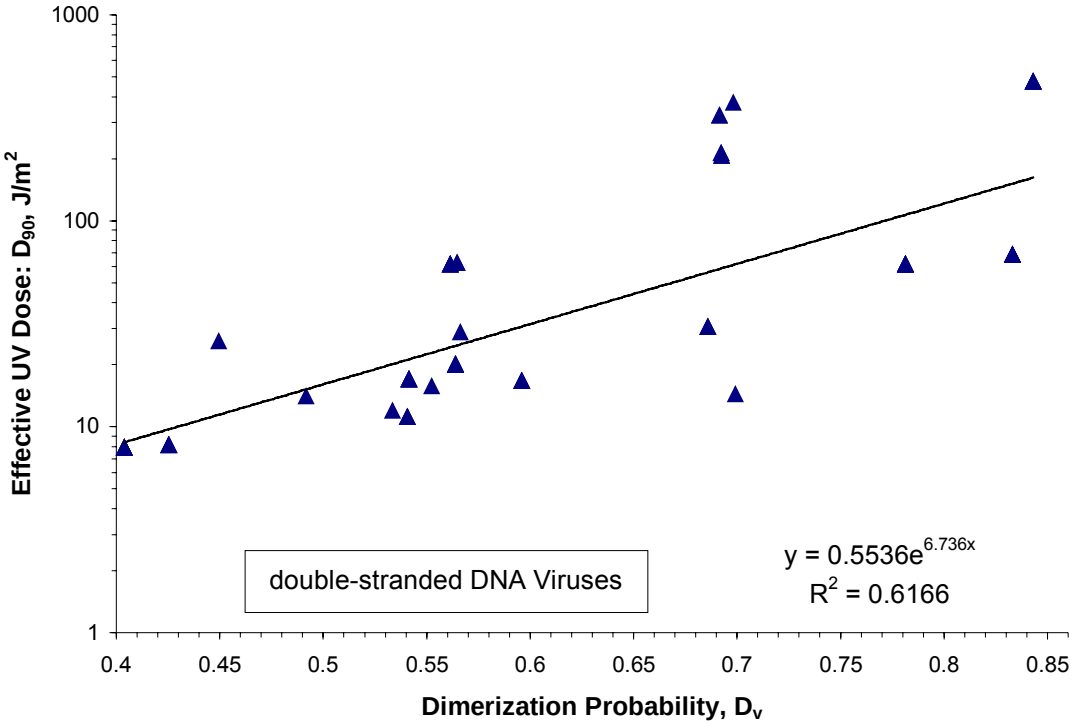

Figure 6: Plot of D_v versus effective UV dose for DNA viruses – the D_{90} is the effective dose because it has been corrected for UV scattering. The line represents a curve fit (equation shown on graph). A total of 77 data sets were used, weighted in the curve fit of the 22 viruses.

The lower R^2 value may be due to the previously mentioned factor of size – DNA viruses are larger than RNA viruses and may have more innate photoprotection. No available data was omitted from Figure 5 other than a few redundant data sets that were unavailable and the only real outliers are the four Adenovirus sets at about D_v=0.7. Adenovirus is unusually resistant to UV and may have a chromophore-rich envelope to protect the DNA from UV damage or may have robust photorepair mechanisms. Adenoviruses also have hemagglutinins on their outer surfaces that may cause them to clump or aggregate. The aggregation of cells or virions can drastically affect the absorbance through scattering of the incident light (Smith and Hanawalt 1969). Future research on such outliers may provide insight into photoprotection that will lead to improved models of UV susceptibility.

Table 6 compares the published estimates of the relative proportions of the various dimer types with the values used in the previous models. The factors shown in the table are the three constants in equations (7) and (16). The best fit constants are those that were used in the model in the previous Figures. The zero values assumed for the constants that were not given by the indicated sources did not have any great influence of the R^2 value. The hyperchromicity factor was zero for all RNA models, and kept at 0.67 for all DNA models. The

results for the DNA model are shown with and without corrections for UV scattering, which make about an 12% difference in the DNA model, but had only a 1% difference on the RNA model, as would be expected from their size. Hyperchromicity had no effect on the RNA model but produced a 1% improvement in the DNA model.

Table 6: Comparison of Dimerization Proportionality Constants

Dimer	Dimer Ratio	Factor	Setlow 1966	Meistrich 1970	Lamola 1973	Unrau 1973	Patrick 1977	Best Fit	
								RNA	DNA
TT	1	1	1	1	1	1	1	1	1
CT	CT/TT	F_A	0.25	0.8	0.8	0.5	1	0.1	0.05
CC	CC/TT	F_B	0.13	0.2	0.2	0.5	1	6	40
UYY	UYY/TT	F_C	0	0	0	0	0	6	18
RNA Model R^2 (NS)			61%	60%	60%	64%	62%	66%	-
RNA Model R^2			**59%**	**61%**	**61%**	**64%**	**62%**	**67%**	-
Hyperchromicity		H	0.67	0.67	0.67	0.67	0.67	0	0.67
DNA Model R^2 (NS)			33%	33%	33%	36%	39%	-	50%
DNA Model R^2 (NH)			41%	44%	44%	48%	51%	-	61%
DNA Model R^2			**43%**	**46%**	**46%**	**50%**	**53%**	-	**62%**

(NH): No hyperchromicity. (NS): UV scattering not included.

Conclusions

A mathematical model has been presented for the prediction of UV susceptibility of RNA and DNA viruses based on base-counting of potential dimers in the virus genomes. The results correlate well with available data on UV rate constants. This model has been used to estimate the UV rate constants for a range of pathogenic animal viruses and bioweapon agents for which complete genomes were available from the NCBI database and Table 7 summarizes these predictions. Minimum and maximum D_{90} values are listed that are within the confidence intervals (CIs) of 86% for DNA viruses and 93% for RNA viruses. These CIs represent only the intervals of the data as summarized and do not include any uncertainty in the original 147 data sets, most of which included no error analysis. These rate constant predictions remain to be corroborated by future laboratory testing. Future research will include application of the DNA model to bacteria. Although this genomic model is based on UV rate constants in water it has a direct bearing on airborne UV rate constants as well, since by establishing a theoretical basis for the UV susceptibility of viruses in water, it becomes possible to link them to airborne rate constants – water-based rate constants represent a limit towards which airborne rate constants converge in high humidity (Peccia et al 2001). The variation of UV rate constants with relative humidity (RH) in air is also a function of the DNA conformation which, in turn, determines the relative ratios of pyrimidine dimers, and so a more fundamental understanding of RH effects, and a testable model, may now be possible. Future research into a more complete model of virus inactivation that addresses the photoprotective effects of UV scattering and UV absorption by viral envelopes and nucleocapsids may lead to even greater predictive accuracy. The limits of

accuracy of the present model may also be improved as more genomes and data on UV rate constants become available, and as more precise UV experiments are performed using collimated beam systems, and the authors hope that researchers will be inclined to either challenge or confirm the predictions in Table 7. If the latter is the case, this model may ultimately enable UV susceptibilities of dangerous pathogens to be determined without the risk of handling them in laboratory tests. The novel approach developed for this research, the use of base-counting software to establish dimerization probabilities, may also have applications in fields unrelated to air and water disinfection, such as ultraviolet photochemistry, mutation research, and solar mutagenesis or skin cancer research.

Table 3: Predicted UV Rate Constants and D_{90} Values

Virus	Type	NCBI #s	Dia. μm	Genome bp	Dimer Prob D_v	UV k m^2/J	UV Dose D_{90}, J/m^2		
							Mean	Min	Max
Camelpox	DNA	NC_003391	0.307	205719	0.3968	0.1280	18	9.6	40
Canine Distemper	DNA	NC_001921	0.173	15690	0.6958	0.0182	126	38	442
Chikungunya	RNA	NC_004162	0.06	11826	0.2161	0.0763	30	9.7	66
Crimean-Congo	RNA	NC_005300,01,02	0.09	19146	0.1947	0.1261	18	6.6	37
Dengue Fever Type 1	RNA	NC_001477	0.045	10735	0.2117	0.0996	23	7.5	49
Dengue Fever Type 2	RNA	NC_001474	0.045	10723	0.2080	0.1146	20	6.9	44
Dengue Fever Type 3	RNA	NC_001475	0.045	10707	0.2091	0.1113	21	7.2	45
Dengue Fever Type 4	RNA	NC_002640	0.045	10649	0.2125	0.0946	24	7.7	51
Ebola (Reston)	RNA	NC_004161	0.09	18891	0.2043	0.0957	24	8.3	51
Ebola (Sudan)	RNA	NC_006432	0.09	18875	0.2066	0.0867	27	8.8	53
Ebola (Zaire)	RNA	NC_002549	0.09	18959	0.2035	0.0991	23	8.3	50
EEE	RNA	NC_003899	0.062	11675	0.2222	0.0613	38	12	83
Fowl Adenovirus A	DNA	NC_001720	0.08	43804	0.6479	0.0349	66	33	220
Fowlpox	DNA	NC_002188	0.307	288539	0.3652	0.1564	15	7.7	30
Goatpox	DNA	NC_004003	0.307	149599	0.3987	0.1232	19	10	40
Hantaan	RNA	NC_005218,19,22	0.095	11845	0.2086	0.0811	28	9.9	63
Hepatitis C	DNA	NC_009827	0.06	9628	0.8542	0.0099	233	110	1097
Herpesvirus Type 4	DNA	NC_009334	0.122	172764	0.5879	0.0436	53	25	157
Herpesvirus Type 6A	DNA	NC_001664	0.1	159322	0.4626	0.1103	21	11	50
Herpesvirus Type 7	DNA	NC_001716	0.155	153080	0.4459	0.1024	22	12	49
Japanese Encephalitis	RNA	NC_001437	0.045	10976	0.2163	0.0860	27	8.9	61
Junin	RNA	NC_005080,81	0.12	10525	0.2304	0.0341	68	21	154
Lassa	RNA	NC_004296,97	0.12	10681	0.2294	0.0372	62	20	107
LCM	RNA	NC_004291,94	0.126	10056	0.2226	0.0430	54	17	118
Machupo	RNA	NC_005079,78	0.11	10635	0.2326	0.0334	69	22	156
Marburg	RNA	NC_001608	0.039	19111	0.1999	0.1654	14	5.0	30
Monkeypox	DNA	NC_003310	0.307	196858	0.3998	0.1232	19	10	40
Mousepox	DNA	NC_004105	0.307	209771	0.3951	0.1247	18	9.8	40
Mumps	RNA	NC_002200	0.245	15384	0.2133	0.0486	47	15	97
Myxoma	DNA	NC_001132	0.25	161766	0.4451	0.0924	25	13	54
Norwalk	RNA	NC_001959	0.032	7654	0.2416	0.0410	56	14	132
Papillomavirus	DNA	NC_001691	0.055	7184	0.7302	0.0236	98	45	369
Parainfluenza Type 1	RNA	NC_003461	0.194	15600	0.1961	0.0968	24	8.6	50
Respiratory Syncytial	RNA	NC_001803	0.19	15225	0.2006	0.0823	28	9.7	58
Rhinovirus B	RNA	NC_001490	0.023	7212	0.2355	0.0526	44	12	99
Rhinovirus C	RNA	NC_009996	0.023	7099	0.2428	0.0417	55	15	125
Rubella	RNA	NC_001545	0.061	9755	0.2634	0.0152	152	37	345
Sendai	RNA	NC_001522	0.194	15384	0.2040	0.0740	31	11	66
Smallpox	DNA	NC_001611	0.307	185578	0.4041	0.1202	19	10	42
Turkey Adenovirus A	DNA	NC_001958	0.08	26263	0.6030	0.0473	49	24	148
Usutu	RNA	NC_006551	0.051	11066	0.2206	0.0693	33	10	73
Yellow Fever	RNA	NC_002031	0.045	10862	0.2151	0.0860	27	8.5	56

References

Aaronson SA. 1970. Effect of ultraviolet irradiation on the survival of simian virus 40 functions in human and mouse cells. J Virol 6(4):393-399.

Abraham G. 1979. The effect of ultraviolet radiation on the primary transcription of Influenza virus messenger RNAs. Virol 97:177-182.

Albrecht T. 1974. Multiplicity reactivation of human cytomegalovirus inactivated by ultra-violet light. Biochim Biophys Acta 905:227-230.
Balch WM, Vaughn J, Novotny J, Drapeau D, Vaillancourt R, Lapierre J, Ashe A. 2000. Light scattering by viral suspensions. Limnol Oceanogr 45(2):492-498.
Battigelli D, Sobsey M, Lobe D. 1993. The inactivation of hepatitis A virus and other model viruses by UV irradiation. Wat Sci Technol 27:339.
Bay PHS, Reichman ME. 1979. UV inactivation of the biological activity of defective interfering particles generated by Vesicular Stomatitis virus. J Virol 32(3):876-884.
Becker MM, Wang Z. 1989. Origin of ultraviolet damage in DNA. J Mol Biol 210:429-438.
Benzer S. 1952. Resistance to ultraviolet light as an index to the reproduction of bacteriophage. J Bact 63:59-72.
Bister K, Varmus HE, Stavnezer E, Hunter E, Vogt PK. 1977. Biological and biochemical studies on the inactivation of Avian Oncoviruses by ultraviolet irradiation. Virol(689-704).
Bockstahler LE, Lytle CD, Stafford JE, Haynes KF. 1976. Ultraviolet enhanced reactivation of a human virus: Effect of delayed infection. Mutat Res 35:189-198.
Bohren C, Huffman D. 1983. Absorption and Scattering of Light by Small Particles. New York: Wiley & Sons.
Bohrerova Z, Shemer H, Lantis R, Impellitteri C, Linden K. 2008. Comparative disinfection efficiency of pulsed and continuous-wave UV irradiation technologies. Wat Res 42:2975-2982.
Bossart W, Nuss DL, Paoletti E. 1978. Effect of UV irradiation on the expression of Vaccinia virus gene products synthesized in a cell-free system coupling transcription and translation. J Virol 26(3):673-680.
Bourre F, Benoit A, Sarasin A. 1989. Respective Roles of Pyrimidine Dimer and Pyrimidine (6-4) Pyrimidone Photoproducts in UV Mutagenesis of Simian Virus 40 DNA in Mammalian Cells. J Virol 63(11):4520-4524.
Butkus MA, Labare MP, Starke JA, Moon K, Talbot M. 2004. Use of aqueous silver to enhance inactivation of coliphage MS-2 by UV disinfection. Appl Environ Microbiol 70(5):2848-2853.
Collier LH, McClean D, Vallet L. 1955. The antigenicity of ultra-violet irradiated vaccinia virus. J Hyg 53(4):513-534.
Cornelis JJ, Su ZZ, Ward DC, Rommelaere J. 1981. Indirect induction of mutagenesis of intact parvovirus H-1 in mammalian cells treated with UV light or with UV-irradiated H-1 or simian virus 40. Proc Natl Acad Sci 78(7):4480-4484.
Danner K, Mayr A. 1979. In vitro studies on Borna virus. II. Properties of the virus. Arch Virol 61:261-271.
Darnell MER, Subbarao K, Feinstone SM, Taylor DR. 2004. Inactivation of the coronavirus that induces severe acute respiratory syndrome, SARS-CoV. J Virol Meth 121:85-91.
David HL. 1973. Response of mycobacteria to ultraviolet radiation. Am Rev Resp Dis 108:1175-1184.
Davidovich IA, Kishchenko GP. 1991. The shape of the survival curves in the inactivation of viruses. Mol Gen, Microb & Virol 6:13-16.
de Roda Husman AM, Bijkerk P, Lodder W, Berg Hvd, Pribil W, Cabaj A, Gehringer P, Sommer R, Duizer E. 2004. Calicivirus Inactivation by Nonionizing (253.7-Nanometer-Wavelength [UV]) and Ionizing (Gamma) Radiation. Appl Environ Microbiol 70(9):5089-5093.
DeFendi V, Jensen F. 1967. Oncogenicity by DNA tumor viruses. Science 157:703-705.
DiStefano R, Burgio G, Ammatuna P, Sinatra A, Chiarini A. 1976. Thermal and ultraviolet inactivation of plaque purified measles virus clones. G Batteriol Virol Immunol 69:3-11.
Dubunin NP, Zasukhina GD, Nesmashnova VA, Lvova GN. 1975. Spontaneous and Induced Mutagenesis in Western Equine Encephalomyelitis Virus in Chick Embryo Cells with Different Repair Activity. Proc Nat Acad Sci 72(1):386-388.
Durance CS, Hoffman R, Andrews RC, Brown M. 2005. Applications of Ultraviolet Light for Inactivation of Adenovirus. : University of Toronto Department of Civil Engineering.
Fluke DJ, Pollard EC. 1949. Ultraviolet action spectrum of T1 bacteriophage. Science 110:274-275.
Freeman AG, Schweikart KM, Larcom LL. 1987. Effect of ultraviolet radiation on the Bacillus

subtilis phages SPO2c12, SPP1, and phi 29 and their DNAs. Mut Res 184(3):187-196.
Furuse K, Watanabe I. 1971. Effects of ultraviolet light (UV) irradiation on RNA phage in H2O and in D2O. Virol 46:171-172.
Galasso GJ, Sharp DG. 1965. Effect of particle aggregation on the survival of irradiated Vaccinia virus. J Bact 90(4):1138-1142.
Garcia-Lopez A, Snider A, Garcia-Rubio L. 2006. Rayleigh-Debye-Gans as a model for continuous monitoring of biological particles: Part I, assessment of theoretical limits and approximations. Optics Express 14(19):17.
Gerba C, Gramos DM, Nwachuku N. 2002. Comparative inactivation of enteroviruses and adenovirus 2 by UV light. Appl Environ Microbiol 68(10):5167-5169.
Golde A, Latarjet R, Vigier P. 1961. Isotypical interference in vitro by Rous virus inactivated by ultraviolet rays. C R Acad Sci (Paris) 253:2782-2784.
Guillemain B, Mamoun R, Astier T, Duplan J. 1981. Mechanisms of early and late polykaryocytosis induced by the Bovine Leukaemia virus. J Gen Virol 57:227-231.
Gurzadyan GG, Nikogosyan DN, Kryukov PG, Letokhov VS, Balmukhanov TS, Belogurov AA, Zavilgelskij GB. 1981. Mechanism of high power picosecond laser UV inactivation of viruses and bacterial plasmids. Photochem Photobiol 33:835-838.
Harm W. 1968. Effects of dose fractionation on ultraviolet survival of *Escherichia coli*. Photochem & Photobiol 7:73-86.
Havelaar AH. 1987. Virus, bacteriophages and water purification. Vet Q 9(4):356-360.
Helentjaris T, Ehrenfeld E. 1977. Inhibition of host cell protein synthesis by UV-inactivated poliovirus. J Virol 21(1):259-267.
Hill WF, Hamblet FE, Benton WH, Akin EW. 1970. Ultraviolet devitalization of eight selected enteric viruses in estuarine water. Appl Microb 19(5):805-812.
Hollaender A, Oliphant JW. 1944. The inactivating effect of monochromatic ultraviolet radiation on influenza virus. J Bact 48(4):447-454.
Hotz G, Mauser R, Walser R. 1971. Infectious DNA from coliphage T1. 3. The occurrence of single-strand breaks in stored, thermally-treated and UV-irradiated molecules. Int J Radiat Biol Relat Stud Phys Chem Med 19:519-536.
Hoyle F, Wickramasinghe C. 1983. The ultraviolet absorbance spectrum of coliform bacteria and its relationship to astronomy. Astrophysics and Space Science 95:227-231.
Kariwa H, Fujii N, Takashima I. 2004. Inactivation of SARS coronavirus by means of povidone-iodine, physical conditions, and chemical reagents. Jpn J Vet Res 52(3):105-112.
Kelloff G, Aaronson SA, Gilden RV. 1970. Inactivation of Murine Sarcoma and Leukemia viruses by ultra-violet irradiation. Virol 42:1133-1135.
Klein B, Filon AR, vanZeeland AA, vanderEb AJ. 1994. Survival of UV-irradiated vaccinia virus in normal and xeroderma pigmentosum fibroblasts; evidence for repair of UV-damaged viral DNA. Mutat Res 307(1):25-32.
Klenin V. 1965. The problem concerning the scattering of light by suspensions of bacteria. Biofizika 10(2):387-388.
Ko G, Cromenas TL, Sobsey MD. 2005. UV inactivation of adenovirus type 41 measured by cell culture mRNA RT-PCR. Wat Res 39:3643-3649.
Lamola A. 1973. Photochemistry and structure in nucleic acids. Pure Appl Chem 34(2):281-303.
Latarjet R, Cramer R, Montagnier L. 1967. Inactivation, by UV-, X-, and gamma-radiations, of the infecting and transforming capacities of polyoma virus. Virol 33:104-111.
Lee JE, Zoh KD, Ko GP. 2008. Inactivation and UV disinfection of Murine Norovirus with TiO2 under various environmental conditions. Appl Environ Microbiol 74(7):2111-2117.
Levinson W, Rubin R. 1966. Radiation studies of avian tumor viruses and of Newcastle disease virus. Virol 28:533-542.
Linden KG, Thurston J, Schaefer R, Malley JP. 2007. Enhanced UV inactivation of Adenoviruses under polychromatic UV lamps. Appl Environ Microbiol 73(23):7571-7574.
Lovinger GG, Ling HP, Gilden RV, Hatanaka M. 1975. Effect of UV light on RNA directed DNA polymerase activity of murine oncornaviruses. J Virol 15:1273.
Lytle CD. 1971. Host-cell reactivation in mammalian cells. 1. Survival of ultra-violet-irradiated herpes virus in different cell-lines. Int J Radiat Biol Relat Stud Phys Chem Med 19(4):329-337.
Mamane-Gravetz H, Linden KG, Cabaj A, Sommer R. 2005. Spectral sensitivity of *Bacillus*

subtilis spores and MS2 coliphage for validation testing of ultraviolet reactors for water disinfection. Environ Sci Technol 39:7845-7852.
Martin JP, Aubertin AM, Kirn A. 1982. Expression of Frog Virus 3 early genes after ultraviolet irradiation. Virol 122:402-410.
Matallana-Surget S, Meador J, Joux F, Douki T. 2008. Effect of the GC content of DNA on the distribution of UVB-induced bipyrimidine photoproducts. Photochem Photobiol Sci 7:794-801.
Meistrich M, Lamola AA, Gabbay E. 1970. Sensitized photoinactivation of bacteriophage T4. Photochem Photobiol 11(3):169-178.
Meng QS, Gerba CP. 1996. Comparative inactivation of enteric Adenoviruses, Poliovirus and coliphages by ultraviolet irradiation. Wat Res 30(11):2665-2668.
Mullaney P, Dean P. 1970. The small angle light scattering fo biological cells. Biophys J 10:764-772.
NCBI. 2009. Entrez Genome. : National Center for Biotechnology Information.
Nomura S, Bassin RH, Turner W, Haapala DK, Fischinger PJ. 1972. Ultraviolet inactivation of Maloney Leukaemia Virus: Relative target size required for virus replication and rescue of 'defective' Murine Sarcoma virus. J Gen Virol 14:213-217.
Nuanualsuwan S, Mariam T, Himathongkham S, Cliver DO. 2002. Ultraviolet inactivation of Feline Calicivirus, Human Enteric Viruses, and coliphages. Photochem Photobiol 76(4):406-410.
Nwachuku N, Gerba CP, Oswald A, Mashadi FD. 2005. Comparative Inactivation of Adenovirus Serotypes by UV Light Disinfection. Appl Environ Microbiol 71(9):5633-5636.
Otaki M, Okuda A, Tajima K, Iwasaki T, Kinoshita S, Ohgaki S. 2003. Inactivation differences of microorganisms by low pressure UV and pulsed xenon lamps. Wat Sci Technol 47(3):185-190.
Owada M, Ihara S, Toyoshima K. 1976. Ultraviolet inactivation of Avian Sarcoma viruses: Biological and Biochemical analysis. Virol 69:710-718.
Patrick MH. 1977. Studies on thymine-derived UV photoproducts in DNA - I. Formation and biological role of pyrimidine adducts in DNA. Photochem Photobiol 25(4):357-372.
Peak MJ, Peak JG. 1978. Action spectra for the ultraviolet and visible light inactivation of phage T7: Effect of host-cell reactivation. Radiat Res 76:325-330.
Peccia J, Werth HM, Miller S, Hernandez M. 2001a. Effects of relative humidity on the ultraviolet induced inactivation of airborne bacteria. Aerosol Sci & Technol 35:728-740.
Petukhov V. 1964. The feasibility of using the Mie theory for the scattering of light from suspensions of spherical bacteria. Biofizika 10(6):993-999.
Rahn RO, Hosszu JL. 1969. Influence of relative humidity on the photochemistry of DNA films. Biochim Biophys Acta 190:126-131.
Rainbow AJ, Mak S. 1970. Functional Heterogeneity of Virions in Human Adenovirus Types 2 and 12. J Vir 5:188-193.
Rainbow AJ, Mak S. 1973. DNA damage and biological function of human adenovirus after U.V. irradiation. Int J Radiat Biol 24(1):59-72.
Rauth AM. 1965. The physical state of viral nucleic acid and the sensitivity of viruses to ultraviolet light. Biophysical Journal 5:257-273.
Rice P, Longden I, Bleasby A. 2000. EMBOSS: The European Molecular Biology Open Software Suite. Trends Genet 16:276-277.
Ronto G, Gaspar S, Berces A. 1992. Phages T7 in biological UV dose measurement. Photochem Photobiol 12:285-294.
Ross LJN, Wildy P, Cameron KR. 1971. Formation of small plaques by Herpes viruses irradiated with ultraviolet light. Virol 45:808-812.
Ryan D, Rainbow A. 1986. Comparative studies of host-cell reactivation, cellular capacity and enahnced reactivation of herpes simplex virus in normal, xeroderma pigmentosum and Cockayne syndrome fibroblasts. Mut Res 166:99-111.
Sarasin AR, Hanawalt PC. 1978. Carcinogens enhance survival of UV-irradiated simian virus 40 in treated monkey kidney cells: Induction of a recovery pathway? Proc Natl Acad Sci 75(1):356-350.
Scholes CP, Hutchinson F, Hales HB. 1967. Ultraviolet-induced damage to DNA independent of molecular weight. J Mol Biol 24:471-474.

Seemayer NH. 1973. Analysis of minimal functions of Simian virus 40. J Virol 12(6):1265-1271.
Sellers MI, Nakamura R, Tokunaga T. 1970. The effects of ultraviolet irradiation on Mycobacteriophages and their infectious DNAs. J Gen Virol 7(3):233-247.
Selsky C, Weichselbaum R, Little JB. 1978. Defective host-cell reactivation of UV-irradiated Herpes Simplex virus by Bllom's Syndrome skin fibroblasts. In: Hanawalt PC, Friedberg EC, Cox CF, editors. DNA Repair Mechanisms. New York: Academic Press.
Setlow RB, Carrier WL. 1966. Pyrimidine dimers in ultraviolet-irradiated DNA's. J Mol Biol 17:237-254 (missing 250-254).
Setlow J, Boling M. 1972. Bacteriophage of *Haemophilus influenzae* - II. Repair of ultraviolet-irradiated phage DNA and the capacity of irradiated cells to make phage. J Mol Biol 63:349-362.
Shanley JD. 1982. Ultraviolet irradiation of Murine Cytomegalovirus. J Gen Virol 63:251-254.
Shimizu A, Shimizu N, Tanaka A, Jinno-Oue A, Roy B, Shinagawa M, Ishikawa O, Hoshino H. 2004. Human T-cell leukaemia virus type 1 is highly sensitive to UV-C light. J Gen Virol 85:2397-2406.
Shin G, Linden KG, Sobsey MD. 2005. Low pressure ultraviolet inactivation of pathogenic enteric viruses and bacteriophages. J Environ Eng Sci 4(Supp 1):S7-S11.
Simonet J, C G. 2006. Inactivation and genome degradation of poliovirus 1 and F-specific RNA phages and degradation of their genomes by UV irradiation at 254 nanometers. Appl Environ Microbiol 72(12):7671-7677.
Smirnov Y, Kapitulez S, Kaverin N. 1992. Effects of UV-irradiation upon Venezuelan equine encephalomyelitis virus. Virus Res 22(2):151-158.
Smith KC, Hanawalt PC. 1969. Molecular Photobiology: Inactivation and Recovery. New York: Academic Press.
Sommer R, Pribil W, Appelt S, Gehringer P, Eschweiler H, Leth H, Cabaj A, Haider T. 2001. Inactivation of bacteriophages in water by means of non-ionizing (UV 253.7nm) and ionizing (gamma) radiation: A comparative approach. Wat Res 35(13):3109-3116.
Stramski D, Keifer D. 1991. Light scattering by microorganisms in the open ocean. Prog Oceanogr 28:343-383.
Templeton MR, Andrews RC, Hofmann R. 2006. Impact of iron particles in groundwater on the UV inactivation of bacteriophages MS2 and T4. J Appl Microbiol 101(3):732-741.
Thurston-Enriquez JA, Haas CN, Jacangelo J, Riley K, Gerba CP. 2003. Inactivation of Feline calicivirus and Adenovirus Type 40 by UV radiation. Appl Environ Microbiol 69(1):577-582.
Unrau P, Wheatcroft R, Cox B, Olive T. 1973. The formation of pyrimidine dimers in the DNA of fungi and bacteria. Biochim Biophys Acta 312:626-632.
van der Eb AJ, Cohen JA. 1967. The effect of UV-irradiation on the plaque-forming ability of single- and double-stranded polyoma virus DNA. Biochem Biophys Res Comm 28(2):284-293.
vandeHulst H. 1957. Light Scattering by Small Particles. New York: Chapman & Hall, Ltd.
VonBrodrotti HS, Mahnel H. 1982. Comparative studies on susceptibility of viruses to ultraviolet rays. Zbl Vet Med B 29:129-136.
Wang SY. 1964. The mechanism for frozen aqueous solution irradiation of pyrimidines. Photochem Photobiol 3:395-398.
Wang J, Mauser A, Chao SF, Remington K, Treckmann R, Kaiser K, Pifat D, Hotta J. 2004. Virus inactivation and protein recovery in a novel ultraviolet-C reactor. Vox Sang 86(4):230-238.
Webb SJ. 1965. Bound Water in Biological Integrity. Springfield, IL: Charles C. Thomas.
Weidenmann A, Fischer B, Straub U, Wang C-H, Flehmig B, Schoenen D. 1993. Disinfcetion of Hepatitis A virus and MS-2 coliphage in water by ultraviolet irradiation: Comparison of UV-susceptibility. Wat Sci Technol 27(3-4):335-338.
Weigle JJ. 1953. Induction of mutations in a bacterial virus. Proc Natl Acad Sci USA 39:628.
Weiss M, Horzinek MC. 1986. Resistance of Berne virus to physical and chemical treatment. Vet Microbiol 11:41-49.
Wilson B, Roessler P, vanDellen E, Abbaszadegan M, Gerba C. Coliphage MS-2 as a UV water disinfection efficacy test surrogate for bacterial and viral pathogens. In: Association

AWW, editor; 1992; Denver, CO.
Winkler U, Johns HE, Kellenberger E. 1962. Comparative study of some properties of bacteriophage T4D irradiated with monochromatic ultraviolet light. Virol 18:343-358.
Wolff MH, Schneweis KE. 1973. UV inactivation of herpes simplex viruses, types 1 and 2. Zentralbl Bakteriol 223(4):470-477.
Yoshikura H. 1971. Ultraviolet inactivation of murine leukemia and sarcoma viruses. Int J Cancer 7:131-140.
Yoshikura H. 1989. Thermostability of Human Immunodeficiency virus (HIV-1) in a Liquid Matrix is far higher than that of an ecotropic Murine Leukemia virus. Jpn J Cancer Res 80:1-5.
Zavadova Z, Gresland L, Rosenbergova M. 1968. Inactivation of single- and double-stranded ribonucleic acid of encephalomyocarditis virus by ultraviolet light. Acta Virol 12:515-522.
Zavadova Z, Libikova H. 1975. Comparison of the sensitivity to ultraviolet irradiation of reovirus 3 and some viruses of the Kemerovo group. Acta Virol 19:88-90.